npg

Vaccinia virus anti-apoptotic F1L is a novel Bcl-2-like domain-swapped dimer that binds a highly selective subset of BH3-containing death ligands

M Kvansakul[1], H Yang[1], WD Fairlie[1], PE Czabotar[1], SF Fischer[1], MA Perugini[2], DCS Huang[1] and PM Colman*,[1]

Apoptosis is an important part of the host's defense mechanism for eliminating invading pathogens. Some viruses express proteins homologous in sequence and function to mammalian pro-survival Bcl-2 proteins. Anti-apoptotic F1L expressed by vaccinia virus is essential for survival of infected cells, but it bears no discernable sequence homology to proteins other than its immediate orthologues in related pox viruses. Here we report that the crystal structure of F1L reveals a Bcl-2-like fold with an unusual N-terminal extension. The protein forms a novel domain-swapped dimer in which the α1 helix is the exchanged domain. Binding studies reveal an atypical BH3-binding profile, with sub-micromolar affinity only for the BH3 peptide of pro-apoptotic Bim and low micromolar affinity for the BH3 peptides of Bak and Bax. This binding interaction is sensitive to F1L mutations within the predicted canonical BH3-binding groove, suggesting parallels between how vaccinia virus F1L and myxoma virus M11L bind BH3 domains. Structural comparison of F1L with other Bcl-2 family members reveals a novel sequence signature that redefines the BH4 domain as a structural motif present in both pro- and anti-apoptotic Bcl-2 members, including viral Bcl-2-like proteins.
Cell Death and Differentiation (2008) **15,** 1564–1571; doi:10.1038/cdd.2008.83; published online 13 June 2008

In higher organisms, programmed cell death (apoptosis) is a prominent feature of the response to viral infection. The central role of the Bcl-2 protein family in maintaining cell survival or driving apoptosis, thereby removing infected, damaged or unwanted cells, is reflected by the expression of sequence, structural and functional orthologues of Bcl-2 by certain viruses.[1] The Bcl-2-related proteins share the presence of one or more of four Bcl-2 homology (BH) domains in their primary sequences and act either to promote cell survival or to counter this.[2] Pro-survival family members such as mammalian Bcl-2, Bcl-x_L, Bcl-w, Mcl-1 and A1 block apoptosis until their protective effect is countered by binding of pro-apoptotic BH3-only proteins, such as Bim, Bad or Noxa.[2,3] Pro-survival Bcl-2 proteins contain multiple BH domains, whereas the distantly related BH3-only proteins contain only the α-helical BH3 domain, which binds a receptor-like groove on the pro-survival proteins, thereby inactivating them.[4,5] Upon activation, pro-apoptotic Bax and Bak, which are essential for apoptosis to proceed,[6] oligomerize to cause organellar damage.

The viral Bcl-2-like proteins, including those expressed by adenovirus, Kaposi sarcoma-associated herpesvirus, Epstein–Barr virus (EBV) and γ-herpesvirus 68, are all required for successful viral propagation and/or persistence. However, other viruses express anti-apoptotic proteins that are unrelated by sequence to any known cell death regulator. These include the myxoma virus M11L,[7] cytomegalovirus vMIA[8] and vaccinia virus F1L[9] and E3L.[10] Despite the lack of

sequence similarity, M11L adopts a Bcl-2-like fold.[11] Moreover, the structure of M11L in complex with the BH3 peptide from Bak revealed that the canonical BH3-binding groove is utilized in this interaction, and tests of M11L mutants showed that its anti-apoptotic action relies on binding to Bak and/or Bax, less so to BH3-only proteins.[11] The vaccinia virus N1L protein also displays a Bcl-2-like fold,[12,13] even though, like myxoma virus M11L, its sequence does not resemble that of Bcl-2. Vaccinia virus lacking N1L replicate normally in cell culture, but are attenuated in animal models.[14] The function of N1L is not fully understood, but its three-dimensional fold and ability to bind BH3 peptides suggest a role in modulating apoptosis.[12,13]

Vaccinia virus F1L inhibits the mitochondrial pathway of apoptosis and, when overexpressed in mammalian cells, it localizes via its C-terminal tail to the mitochondria.[9] F1L interacts with the isolated BH3 domain of Bim and an F1L-deficient virus potently causes Bak/Bax-mediated apoptosis.[10] Unlike the parent, this mutant virus fails to block Bak activation triggered by staurosporine. In the absence of any apoptotic stimuli, F1L reportedly binds to endogenous Bak but not to pro-survival Bcl-2 family members.[9,15] F1L also inhibits the activation of Bax and its translocation to mitochondria following an apoptotic stimulus, possibly because it interacts with Bim.[16]

To elucidate at a molecular level how F1L counters apoptosis, we solved by X-ray crystallography the three-dimensional structure of F1L isolated from the modified vaccinia virus Ankara strain (MVA). Unexpectedly, F1L

adopts a Bcl-2-like fold by the formation of an unusual domain-swapped dimer. Our structure provides a rationale for how BH3 domains interact with F1L. Previously, a small region of F1L (residues 64–84) was reported to directly interact with Bak, potentially constituting a 'BH3-like' domain in F1L.[17] This conclusion is incompatible with the structure of F1L we report here.

Results

F1L adopts a domain-swapped Bcl-2-like fold. The crystal structure of F1L reveals that the polypeptide folds into eight helical segments, here labelled $\alpha0$–$\alpha7$ (Figures 1a and 2). The $\alpha1$ helix is swapped[18] into a neighbouring polypeptide that is related by a crystallographic two-fold symmetry axis (Figure 1b). The resulting arrangement of $\alpha1^*$, $\alpha2$–$\alpha7$ forms the helical bundle characteristic of Bcl-2 family proteins,[19] $\alpha1^*$ denoting the helix from the partner polypeptide in the dimer. Bcl-x_L (PDB code 1MAZ) is the closest structural match found by the DALI server and yet it has only 12% sequence identity with F1L over the 129 residues of F1L's Bcl-2-like region. The loop region between $\alpha1$ and $\alpha2$ of F1L is unusually short (2 amino acids) when compared to other monomeric Bcl-2 family members such as Bcl-x_L, where the homologous loop contains ~60 amino acids (Figure 2), suggesting a rationale for the $\alpha1$ domain swap (see below). Pro-survival Bcl-2 family proteins engage BH3 ligands via a hydrophobic groove largely comprising helices $\alpha2$–$\alpha5$. In the F1L structure, hydrophobic amino acids from helices $\alpha2$, $\alpha4$ and $\alpha5$ form such a groove, together with the largely disordered '$\alpha3$' segment, so labelled only for consistency with the Bcl-2 family protein structure.

The N-terminal extension, $\alpha0$, is novel in known Bcl-2 structures. It is folded against the $\alpha5/\alpha6$ corner of its own polypeptide. The N-terminal end of $\alpha0$ partially fills the BH3-binding groove of a neighbouring molecule, forming a network of crystal contacts. No evidence of higher-order oligomers of F1L in solution can be detected (see below), suggesting that this interaction is a crystallographic artefact. A 27-mer peptide corresponding to $\alpha0$ shows no binding to F1L in solution using ITC (data not shown).

The F1L dimer. As in monomeric Bcl-2 family proteins, the $\alpha1$ helix engages on one side in intimate contacts with the core of the helix-bundle fold. Specifically, F1L residues V62, A65, V66, Y69 and M70 from helix $\alpha1^*$ engage in canonical interactions with the core of the Bcl-2-like helix bundle (Y89, I182, V179, F178, I146 and C174). However, in mammalian pro-survival proteins, the other side of helix $\alpha1$ is partially solvent-shielded by the loop connecting to helix $\alpha2$, whereas

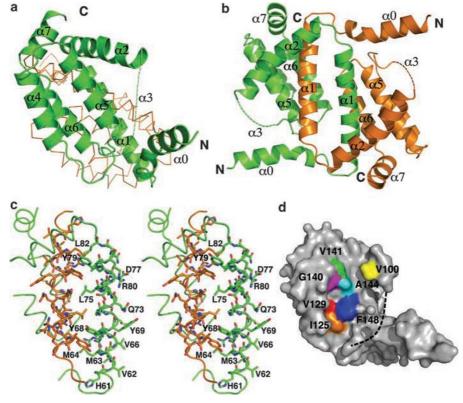**Figure 1** (**a**) Structure of F1L. One monomer is shown as a cartoon (green), with helices 0–7 labelled, and the dotted line indicating the position of the disordered '$\alpha3$' segment. This view looks into the putative BH3-binding grove, which is formed by segments $\alpha2$–$\alpha5$. The second monomer is shown as a trace (orange). (**b**) Structure of the F1L homodimer. Monomeric F1L subunits are shown as a cartoon in green and orange. The view is down the two-fold symmetry axis between the domain-swapped $\alpha1$ helices. (**c**) Stereo-view of the F1L dimer interface. The view is preserved from (**b**). For clarity, only $\alpha1$ is shown for the orange monomer. Important residues in the interface are labelled and shown for the green monomer. (**d**) Molecular surface representation of F1L. The view is preserved from (**a**). F1L residues mutated in the binding assays (Figure 3b) are highlighted in colour. Location of the disordered '$\alpha3$' segment is indicated by a dotted line
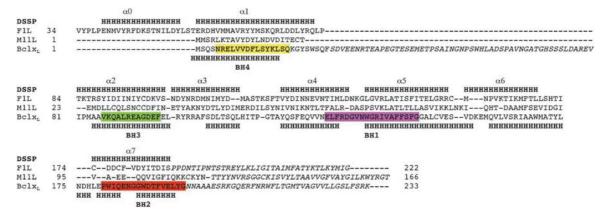
Figure 2 Sequence and structural alignment of F1L with M11L[11] and Bcl-x$_L$.[19] Coloured boxes denote the BH1-4 domains in Bcl-x$_L$. Helices in F1L and Bcl-x$_L$ are marked 'H', and residues in italics were not included when generating the alignment

in F1L it forms the dimer interface through hydrophobic residues that include M64, Y68, L75, Y79 and L82 (Figure 1c). The putative BH3-binding grooves lie on opposite sides of the resulting dimer. Furthermore, in the dimer, the α7 C-terminal helices are approximately parallel, potentially allowing the C-terminal transmembrane segments to anchor the dimer into mitochondrial membranes without occluding either of the BH3-binding sites on the F1L dimmer.

F1L is a dimer in solution. During recombinant protein purification, F1L eluted at a volume commensurate with a dimeric form (data not shown). Sedimentation velocity studies by analytical ultracentrifugation at an initial protein concentration of 1.0 mg/ml revealed a single species with an apparent molar mass of 43 kDa and sedimentation coefficient ($s_{20,w}$) of 3.4 S (Table 1; data not shown). These results support the conclusion that the novel dimeric structure observed in the crystals is not an artefact of crystallization, rather it is a property of the protein in dilute solution. To confirm the role of the length of the α1/α2 loop in dimer formation, we characterized three different Bcl-x$_L$ constructs that lack their C-terminal membrane anchor (Bcl-x$_L$ΔC) by gel filtration, clearly showing that Bcl-x$_L$ΔC consisting of the full cytoplasmic domain and the construct lacking amino acids 45–84 are monomeric in solution, but removal of amino acids 27–82 generates a dimeric form (Figure 4). We confirmed the dimeric state of Bcl-x$_L$ΔC lacking amino acids 27–82 using analytical ultracentrifugation, which revealed a single species with an apparent molar mass of 33 kDa and sedimentation coefficient ($s_{20,w}$) of 3.0 S (Table 1; data not shown). Various attempts to engineer a monomeric form of F1L were unsuccessful (see Supplementary results).

Bcl-2 homology domains. F1L adopts a Bcl-2-like fold, even though at a primary sequence level no homology is detectable to any other member of the Bcl-2 family of proteins. Considering the absence of signature BH domains in F1L, we examined the structural segments in F1L that correspond to the BH domains in other Bcl-2 members. The BH4 domain comprises much of the N-terminal helix (α1) of the eight-helix fold of Bcl-2. Helix α1 packs against elements of α2 (BH3), α5 (BH1) and α8 (BH2), but on the opposite side of the protein to the binding site for exogenous BH3 ligands.

Table 1 Analytical ultracentrifugation of F1L and Bcl-x$_L$

Sample	$s^0_{20,w}$ [a] (S)	M_r [b]	M^c (kDa)	f/f_0 [d]	a/b [e]
F1L	3.4	21 429	42.7	1.35	3.7
Bcl-x$_L$ NL	3	17 901	33	1.31	3.4

[a]Standardized sedimentation coefficient taken from the ordinate maximum of the $c(s)$ distribution (data not shown). [b]Relative monomeric molecular mass (M_r) determined from the amino-acid sequence. [c]Apparent molar mass (M) taken from the ordinate maximum of the $c(M)$ distribution. [d]Frictional coefficient of the dimer calculated using the v-bar method.[38] [e]Axial ratio (a/b) assuming a prolate ellipsoidal structure calculated using the v-bar method.[38]

The structural superposition shows a conserved sequence motif in α1 (Figure 5), comprising $\phi_1 \phi_2$ X X $\phi_3 \phi_4$, where X is any amino acid, ϕ is a hydrophobic residue, $\phi_1 \phi_2$ and ϕ_4 are aliphatic amino acids and ϕ_3 is an aromatic amino acid (Figure 5).

Ligand binding of F1L. BH3-only proteins have been shown to initiate apoptotic signalling in response to a variety of signals, leading to oligomerization of pro-apoptotic Bax and Bak. To gain further insight into the biological role of F1L, we assessed the binding of different BH3 domain peptides from mammalian BH3-only proteins, from the pro-apoptotic proteins Bak and Bax, and from Beclin-1 and Mule (Figure 3a). The results from isothermal calorimetry (Supplementary Figure S1) and from competition and direct binding studies (Figure 3) in a Biacore biosensor are in good agreement. Only a 26-mer peptide spanning Bim BH3 binds tighter than 1 μM to F1L, the K_d being 250 nM (Figure 3a and Supplementary Figure S1). Unexpectedly, F1L does not measurably interact with a 26-mer Bak BH3 peptide, as revealed by the Biacore (S51) direct binding assay, whereas a 28-mer Bax BH3 binds weakly with a K_d of ∼2 μM. However, using isothermal calorimetry, we were able to measure binding of a 26-mer Bak BH3 peptide with a K_d of 4.3 μM (Supplementary Figure S1). Failure to express F1L in mammalian cells frustrated our attempts to corroborate these interactions *in vivo*.

Mutagenesis studies. To further characterize the interaction between F1L and BH3 domain peptides, we

a
WT F1L binding to BH ligands

Ligand	K_D (nM)
hsBad	>1000
hsBid	>1000
hsBim	250±142
mmBmf	>1000
mmHrk	>1000
hsNoxa	>1000
hsPuma	>1000
mmMule	>1000
mmBeclin	>1000
hsBak	>1000
hsBax 28-mer	1850±150

b
WT Bim binding to F1L mutants

F1L variants	Bim IC_{50} (nM)
V100A	NB
V100F	314±15
I125A	NB
I125F	34±10
V129L	283±134
G140F	NB
V141F	91±46
V141L	251±51
A144F	103±3
F148A	NB
F148E	NB
WT	230±37

c
WT F1L binding to Bim mutants

Peptide	IC_{50} (nM)
I58A	>10 000
A59E	4000±1000
L62A	>10 000
I65A	>10 000
G66E	>10 000
D67A	290±32
F69A	3185±815
WT	230±37

d
F1L I125F binding to Bim mutants

Peptide	IC_{50} (nM)
I58A	550±96
L62A	4500±805
I65A	1000±185
D67A	70±5
F69A	190±8
WT	34±10

Figure 3 Binding data for F1L and its ligands. (**a**) BH3-binding profile of wild-type (WT) F1L. K_d values were determined by Biacore S51 assays. (**b**) Mutagenesis mapping of F1L binding groove. IC_{50} values shown were measured for mutant F1L binding to WT Bim BH3. (**c**) Binding of mutant Bim BH3 peptides to WT F1L. (**d**) Binding of mutant Bim BH3 peptides to F1L I125F. IC_{50} values for (**b–d**) were determined by competition experiments using the Biacore 3000 system; NB indicates that no binding was detected

Figure 4 Loop-deleted Bcl-x$_L$ runs as a dimer on gel filtration. Purified Bcl-x$_L$ (predicted MW = 23 778), Bcl-x$_L$ with a shortened α1–α2 loop (Bcl-x$_L$-SL, Δaa 45–84, predicted MW = 20 780) and Bcl-x$_L$ with no α1–α2 loop (Bcl-x$_L$-NL, Δaa 27–82, predicted MW = 17 901) were passed over a Sup75 10-300 column equilibrated with 20 mM Tris pH 8.0 and 150 mM NaCl. All proteins lacked the C-terminal transmembrane anchor (ΔC25). Bcl-x$_L$-SL also contained a C-terminal His tag. Bcl-x$_L$, Bcl-x$_L$-SL and Bcl-x$_L$-NL were expressed and purified as described previously[4,21,39]

performed site-directed mutagenesis on F1L and determined the effect of these mutations on Bim binding (Figures 1d and 3b). Mutants V100A, I125A, G140F, F148A and F148E completely abrogated binding. The V100F, V129L and V141L mutations did not significantly impair Bim binding, whereas I125F, V141F and A144F increased F1L affinity for Bim.

We then investigated the effect of mutations in Bim on binding to wild-type F1L (Figure 3c). Substitution of each of the four conserved hydrophobic residues of the Bim BH3 domain with alanine (I58A, L62A, I65A and F69A) compromises binding, as does substitution of the two small amino acids (A59 and G66) with glutamic acid, whereas substitution of aspartic acid (D67) with alanine is tolerated. The F1L mutant I125F, which binds more tightly than wild-type F1L to wild-type Bim BH3, is also sensitive to mutation of the signature BH3 amino acids of Bim (Figure 3d). These results support a similar model for Bim BH3 binding to F1L as it does to Bcl-x$_L$[5] or Mcl-1,[20] but a three-dimensional structure of an F1L:BH3 domain complex is needed to confirm the results.

Discussion

Oligomerization of Bcl-2 family members is intimately associated with apoptosis signalling. To date, structural studies of such oligomers have addressed only the heterodimerization of pro-survival Bcl-2 family members with isolated BH3 domains, but homo-oligomers of Bak and Bax are widely believed to presage apoptosis.[3] This report of the structure of
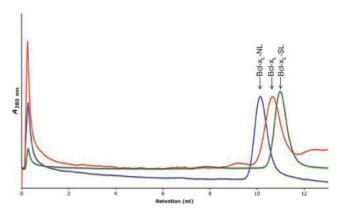
F1L is a novel example of a naturally occurring homodimer of a Bcl-2 family protein. Two examples of domain-swapped homodimers of Bcl-2-like proteins have previously been reported, both for Bcl-x$_L$.[21,22] In one case, a dimer was induced by exposure to alkali, resulting in domain swapping of helices α6–α8.[22] The crystallization of Bcl-x$_L$ with the Beclin BH3 domain[21] displays an α1 domain-swapped dimer, similar but not identical to that reported here for F1L. The dimer in that case was attributed to a crystallization artefact. However, analytical ultracentrifugation and gel-filtration analysis of Bcl-x$_L$ with an identically shortened loop indicate that the protein is a dimer in solution (Figure 4 and Table 1). Thus, α1/α2 loop length can control dimerization of Bcl-2-like proteins. In the F1L structure, α1 is extended (Figure 2) and the connecting loop to α2 is short, both conditions that promote homodimerization by domain swapping. Dimerization driven by swapping of the α1 domains may be of special interest because of the body of data that suggest exposure of the N terminus of Bax and Bak as a signature of their activation.[23,24] N1L also exists as a dimer,[14] but no domain swapping occurs in that case.[12,13]

Other structural studies of Bcl-2 family proteins suggest that the fold is largely unaffected by the presence or absence of the C-terminal membrane anchor. If the C-terminal segments, absent in our construct, are taken into consideration, the dimer structure we describe is compatible with membrane anchoring (see, for example, Figure 1b, and note the dyad-related α7 segments projecting towards the viewer). Furthermore, the dimer structure is compatible with Bim BH3 binding. Bim, like most other BH3-only proteins, is intrinsically unstructured before engagement with a Bcl-2 pro-survival family member.[25] The BH3 domain of Bim is located near its C-terminal membrane anchor,[26] allowing for Bim insertion, in the correct orientation, into the BH3-binding groove of the membrane-anchored F1L dimer. A similar argument for the binding of full-length Bak to F1L[15] is less directly advanced because the Bak BH3 is not exposed in the structure of C-terminally truncated Bak,[27] necessitating some

conformational change to allow its engagement with F1L, or for that matter with either Bcl-x$_L$ or Mcl-1.[28]

Postigo *et al*.[17] observed that the first 56 amino acids (in MVA strain) (that is, up to and including the first two residues of α1) of F1L are not required for suppression of apoptosis. Whether or not they have another function is unclear. Therefore, truncation of the N-terminal residues as described here to obtain soluble expressed protein has no known consequences for apoptosis. Orthologues of F1L in other poxviruses show most variability at the N terminus, but display 95% sequence identity over the C-terminal 220 amino acids.[29] Our alignment of MVA F1L with 12 other orthologues indicates that from MVA F1L residue 16 onwards, the remainder of the sequence is highly conserved within all aligned orthologues (data not shown). The ordered part of our structure commences at residue 34, and thus represents most of the highly conserved region of F1L. Removal of amino acids 61–76 (57–72 in MVA strain) results in loss of apoptosis-suppressing function.[17] These residues comprise most of the α1 helix of F1L, and are essential for the integrity of the structure of the dimer and (probably) of the folded protein. Other mutants of the Western Reserve strain described in that study include M67P and the double mutant V66E/V70E, neither mutant preventing UV-induced cell death. In the MVA strain, the homologous residues are M63, V62 and V66. These residues comprise part of the hydrophobic interface between α1* and the partner domain into which it is swapped (see Figure 1c), and these mutants may well be structurally disruptive.

The absence of a canonical BH3 domain sequence in F1L suggests that its interaction with Bak is more likely to involve the Bak BH3 into the F1L groove rather than the converse. F1L is able to bind BH3 domains of Bim and (more weakly) Bax, and we propose that this interaction is mediated by the putative BH3-binding groove of F1L described above. In mammalian Bcl-2 family members, this groove is formed by structural elements that correspond to the BH1, BH2 and BH3 homology domain sequences, yet no such sequence signatures are evident in F1L. A similar conundrum confronted the explanation for BH3 binding to M11L, but was resolved by a crystal structure of M11L bound to the Bak BH3 domain, supported by mutagenesis and functional analysis.[11] Our mutagenesis studies of the Bim BH3 peptide and F1L, and the associated binding data, support a model in which F1L acts as a receptor for the BH3 domain of the BH3-only protein Bim. The inconsequential effect of the D67A mutation in Bim on this interaction suggests that D67 in Bim may be adjacent to V141 of F1L in the complex. In F1L, V141 is the structural homologue of a conserved arginine in the BH1 domain of mammalian pro-survival proteins (Figure 2). This result is reminiscent of the lack of any effect on binding to myxoma virus M11L when the equivalent D63 residue was mutated.[11] M11L also lacks the conserved arginine residue in the BH1 domain. M11L and F1L are the dominant apoptosis-suppressing proteins in myxoma and vaccinia virus, respectively; they share the Bcl-2-like fold but are themselves only 14% identical in sequence over the Bcl-2-like region of F1L.

The apparent absence of any BH domain in F1L prompted us to examine the structural segments in F1L that correspond to BH domains in other Bcl-2 members. This examination

Figure 5 Novel consensus sequence motif redefining the BH4 domain. The novel BH4 motif is formed by $\phi_1 \phi_2$ X X $\phi_3 \phi_4$, where X is any amino acid, ϕ is a hydrophobic residue and ϕ_3 is an aromatic residue. PDB accession codes[40] are given in parentheses for each structure

uncovered a conserved sequence motif – $\phi_1 \phi_2$ X X $\phi_3 \phi_4$ – for the BH4 domain, where X is any amino acid, $\phi_1 \phi_2$ and ϕ_4 are aliphatic residues and ϕ_3 is an aromatic residue (Figure 5). Some reports claim that pro-apoptotic Bax and Bak have no BH4 domain and the presence or absence of the BH4 domain is a distinguishing feature of the anti- and pro-apoptotic family members,[30] a dogma that permeates much of the current literature and many authoritative reviews.[2] A BH4 signature is evident enough in the sequences of Bcl-2, Bcl-x and Bcl-w, but is more controversial in Mcl-1 and A1. Our structure alignments illustrate the presence of the above motif in helix α1 of Mcl-1, of Bak and Bax, and of viral Bcl-2-like proteins (Figure 5). It appears that there is no basis in the α1 sequence for distinguishing the pro- and anti-apoptotic family members. Furthermore, binding of BH3 peptides to Bcl-x$_L$ and Mcl-1 does not significantly alter the environment of their BH4 domains. We suggest that the BH4 domain as defined here is a structural motif common to the Bcl-2 family fold. A functional role in antagonizing apoptosis signalling *in vivo* has been reported for the peptide corresponding to the BH4 domain of Bcl-x.[31] An inactive BH4 domain in that study was generated by replacing both ϕ_1 and ϕ_2 with glycine.

Interestingly, vaccinia virus appears to contain two functional Bcl-2 like proteins, F1L and N1L. (The sequences of these proteins are only 3% identical over the Bcl-2-like region of F1L.) Vaccinia virus lacking N1L grows normally in culture, but it has an attenuated phenotype in mouse models.[14] N1L reportedly binds BH3 peptides of Bim, Bak and Bid,[12] and interacts with Bad, Bax and Bid in cells transfected with the N1L gene.[13] In contrast, virus lacking F1L (VVΔF1L) results in apoptosis of infected cells in culture,[10,15] suggesting that

anti-apoptotic properties of vaccinia virus are primarily conferred by F1L. By comparison, EBV, which harbours two Bcl-2 sequence homologues BHRF-1 and BALF-1, requires both proteins to establish latent infection and to transform B cells.[32] Thus, BHRF-1 and BALF-1 appear to work in concert. It remains to be seen if both F1L and N1L are required for different stages of an infection caused by vaccinia virus.

F1L exhibits a markedly limited BH3-binding profile compared to mammalian Bcl-2 family members. Bcl-x_L has been shown to interact with numerous BH3-only proteins as well as with Bax and Bak BH3 domains,[33] whereas F1L showed no measurable affinity for most BH3 peptides tested, exceptions being Bim and, to a lesser extent, Bax and Bak (Figure 3a and Supplementary Figure S1). The affinity reported here for Bim is somewhat weaker than the previously reported 75 nM,[10] which may be due to the use of human Bim BH3 peptide in our current study compared to murine Bim BH3 in the previous one. Furthermore, affinity measurements for wild-type F1L with wild-type BH3 peptides in this study were performed as direct binding experiments, thus determining dissociation constants (K_d), whereas previously[10] a competition assay was employed that determined IC_{50} values. Although only very weak binding was detected here to the BH3 peptide from Bak, interaction between F1L and Bak in transfected cells has been observed.[15] This might suggest a synergy deriving from the co-localization of Bak and F1L on the mitochondrial membrane, or the importance of regions of Bak and F1L other than the tongue-in-groove components (for example, the membrane anchoring regions), in the interaction. In contrast, we have measured a weak interaction with the Bax BH3, but no association of F1L with Bax in a cell has been reported, other than following detergent activation of Bax.[16] Instead, experimental evidence supports a role for F1L in blocking activation of Bax in the absence of direct binding to it.[16] It is possible that the weak interaction we describe here between the Bax BH3 and F1L has little or no role in controlling Bax activation. The tighter interaction we describe between Bim BH3 and F1L might explain F1L's antagonism of Bax activation through a sequestration mechanism to prevent Bim binding either directly to Bax or indirectly to Bcl-2 family members.[16] Vaccinia virus-induced apoptosis is reduced in Bim-deficient cells,[16] suggesting that Bim, and potentially other BH3-only proteins, is upregulated or activated in response to infection by vaccinia virus.

The affinities measured for Bim and Bax BH3 domains are modest compared to the low nanomolar affinities reported for most mammalian Bcl-2 members.[33] Nevertheless, VVΔF1L triggers apoptosis, suggesting that F1L is indeed the predominant anti-apoptotic protein expressed by vaccinia virus, despite the low affinity for BH3 ligands. It will be interesting to determine whether or not the dimeric form of F1L contributes to its potent ability to inhibit apoptosis.

The apoptotic machinery has emerged as a promising drug target for cancer therapy following the discovery of organic molecules that can mimic the pro-apoptotic function of certain BH3 domain-containing proteins.[34,35] Similarly, the putative BH3-binding groove of F1L described here may be a valid target for therapies whose mode of action would be to trigger apoptosis in vaccinia virus-infected cells. Although variola

virus is essentially eradicated in the community, concerns persist about its re-emergence as a potential bioweapon.[36]

Materials and Methods

Recombinant protein production. The complete cDNA of F1L MVA was used to amplify by polymerase chain reaction (PCR) the region coding for residues 18–186 of F1L. The forward primers introduced a *Bam*HI restriction site, and the reverse primer introduced a stop codon followed by an *Eco*RI site. The PCR product was cloned into the pET DUET vector (Invitrogen) or pGEX-6P3 vector (GE Healthcare) using *Bam*HI and *Eco*RI, and expressed in *Escherichia coli* BL21 (DE3) pLysS cells. Cells were grown from an overnight culture to an OD_{600} of 1.0–1.2. Protein expression was induced with 500 mM isopropyl-β-D-thiogalactopyranoside for 4 h, after which the cells were pelleted by centrifugation. For protein purification, cell pellets were homogenized using an Avestin EmulsiFlex homogenizer in lysis buffer (20 mM Tris-HCl pH 8.0, 150 mM NaCl, 10 mM 2-mercaptoethanol). Cell lysates containing hexahistidine-tagged F1L were centrifuged and filtered before loading onto a 1 ml Hi-Trap chelating column (GE Healthcare) charged with nickel. The protein was eluted in 50 mM Tris pH 8.0, 150 mM NaCl, 10 mM 2-mercaptoethanol and 250 mM imidazole and subjected to preparative gel-filtration chromatography in 20 mM Hepes pH 7.5, 150 mM NaCl and 10 mM DTT using a Superdex 200 column, where it eluted as a single peak. Cell lysates containing GST-tagged F1L were centrifuged and filtered before loading onto a glutathione Sepharose column (GE Healthcare) and washed with buffer. F1L was eluted with Tris pH 8.0, 150 mM NaCl, 10 mM DTT and 10 mM glutathione, and further purified on a Superdex 200 column in 20 mM Hepes pH 7.5, 150 mM NaCl and 10 mM DTT.

Crystallization and structure determination. Crystals of F1L were grown by the sitting drop method at room temperature in 0.9–1.2 M NaCl and 50 mM Na/K phosphate pH 5.2. The crystals belong to space group P23 with $a = 88.26$ Å. The asymmetric unit contains one protein chain and 54% solvent. Diffraction data were collected from frozen crystals at 100 K using a Raxis 4 + + image plate detector mounted on a Rigaku Micromax 007 rotating anode X-ray generator equipped with an AXCO capillary optics (CuKα radiation $\lambda = 1.54$ Å). Diffraction data were processed with HKL2000. A heavy atom derivative was obtained by soaking crystals in mother liquor supplemented with 1 M NaI for 30 s. Heavy atom sites were found and refined with SHELX. After density modification, a final model was built with Coot[37] and refined with Refmac5. Crystallographic data are summarized in Table 2. The coordinates have been deposited in the Protein Data Bank (accession code 2vty). Figures were prepared using PyMol.

Measurement of dissociation constants. Biacore competition assays were performed as described.[33] Direct binding assays were performed on a Biacore S51. Affinity measurements were performed at room temperature on a Biacore S51 biosensor with 0.15 M NaCl, 3 mM EDTA, 0.005% Surfactant P20, 5% (v/v) DMSO and 0.01 M Hepes pH 7.4 as the running buffer. Anti-GST antibodies (Qiagen) were immobilized on CM5 sensorchips using amine-coupling chemistry. Recombinant F1L (100 μg/ml) was then injected at the flow rate of 10 μl/min and captured via an N-terminal GST. All BH3 domain peptides (Mimotopes) were prepared in running buffer. Several concentrations of peptide around that peptide's K_d were injected at a flow rate of 90 μl/min. Peptides were allowed to associate with the protein for 60 s and dissociation was monitored for 60 s. All sensorgrams were generated using double referencing by subtracting the binding response from a reference spot, followed by corrections for solvent bulk shifts and subtraction of an average of the running buffer only injections over the immobilized spot. For K_d calculation, corrected response data were fitted using a 1:1 binding site model including mass transport limitations.

Analytical ultracentrifugation. Sedimentation velocity experiments were conducted in a Beckman model XL-I analytical ultracentrifuge at a temperature of 20°C. A 380 μl volume of sample (1.0 mg/ml) and 400 μl of reference solution (25 mM KH_2PO_4, 150 mM NaCl, pH 7.5) were loaded into a conventional double sector quartz cell and mounted in a Beckman 4-hole An-60 Ti rotor. Samples were centrifuged at a rotor speed of 40 000 r.p.m. and the data were collected at a single wavelength (275 nm for F1L and 293 nm for Bcl-x_L) in continuous mode, using a time interval of 300 s and a step size of 0.003 cm without averaging. Solvent density (1.007 g/ml at 20°C) and viscosity (1.021 cP), as well as estimates of the partial specific volume (0.723 ml/g for F1L and 0.726 ml/g for Bcl-x_L at 20°C) and hydration

Table 2 Crystallographic statistics

Crystal	F1L native	F1L NaI	F1L high
Data collection and phasing			
Space group	P23	P23	P23
Resolution range (Å)	50–2.9	50–3.2	50–2.1
Unique reflections	5299	3957	13 687
Multiplicity[a]	4.9 (4.2)	7.5 (7.4)	5.1 (5.1)
Completeness (%)[a]	99.8 (100)	99.8	99.4 (99.9)
R_{merge}[a,b]	0.167 (0.479)	0.227	0.090 (0.548)
R_{deriv}[c]		0.212	
R_{cullis} (centric/acentric)		0.653/0.609	
Phasing power (centric/acentric)[e]		1.46/1.39	
Refinement			
Resolution range (Å)			50–2.1
Reflections (working set/test set)			12 940/680
Protein atoms			2065
Solvent atoms			68 H_2O
R_{cryst}/R_{free}[f]			0.192/0.207
r.m.s.d. bonds (Å)			0.017
r.m.s.d. angles (deg)			1.6
Ramachandran plot (%)[g]			97.0/3.0/0.0/0.0

[a]Numbers in parentheses refer to the highest resolution shells. [b]$R_{merge}=\sum_h\sum_i |I_i(h)-\langle I(h)\rangle|/\sum_h\sum_i I_i(h)$, where $I_i(h)$ is the ith measurement of reflection h and $\langle I(h)\rangle$ is the weighted mean of all measurements of h. [c]$R_{deriv}=\sum_h ||F_{PH}|-|F_P||/\sum_h |F_P|$, where F_P and F_{PH} are the native and derivative structure factors, respectively. [d]$R_{cullis}=\sum_h |||F_{PH}|-|F_P||-|F_H||/\sum_h||F_{PH}|-|F_P|$, where F_H is the calculated heavy atom structure factor. [e]Phasing power is defined as (r.m.s. F_H/r.m.s. lack of closure). [f]$R=\sum_h|F_{obs}-F_{calc}|/\sum_h F_{obs}$, where F_{obs} and F_{calc} are the observed and calculated structure factor amplitudes, respectively. R_{cryst} and R_{free} were calculated using the working and test set, respectively. [g]Residues in most favoured, additionally allowed, generously allowed and disallowed regions.

estimate (0.401 g/g for F1L and 0.381 g/g for Bcl-x_L) were computed using the program SEDNTERP.[38] Sedimentation velocity data at multiple time points were fitted to either a non-interacting discrete species model of up to three components or a continuous size-distribution model using the program SEDFIT, which is available at www.analyticalultracentrifugation.com.

1. Cuconati A, White E. Viral homologs of BCL-2: role of apoptosis in the regulation of virus infection. *Genes Dev* 2002; **16**: 2465–2478.
2. Adams JM, Cory S. The Bcl-2 apoptotic switch in cancer development and therapy. *Oncogene* 2007; **26**: 1324–1337.
3. Youle RJ, Strasser A. The BCL-2 protein family: opposing activities that mediate cell death. *Nat Rev Cell Biol* 2008; **9**: 47–59.
4. Sattler M, Liang H, Nettesheim D, Meadows RP, Harlan JE, Eberstadt M et al. Structure of Bcl-x_L–Bak peptide complex: recognition between regulators of apoptosis. *Science* 1997; **275**: 983–986.
5. Liu X, Dai S, Zhu Y, Marrack P, Kappler JW. The structure of a Bcl-x_L/Bim fragment complex: implications for Bim function. *Immunity* 2003; **19**: 341–352.
6. Lindsten T, Ross AJ, King A, Zong W, Rathmell JC, Shiels HA et al. The combined functions of proapoptotic Bcl-2 family members Bak and Bax are essential for normal development of multiple tissues. *Mol Cell* 2000; **6**: 1389–1399.
7. Graham KA, Opgenorth A, Upton C, McFadden G. Myxoma virus M11L ORF encodes a protein for which cell surface localization is critical in manifestation of viral virulence. *Virology* 1992; **191**: 112–124.
8. Goldmacher VS, Bartle LM, Skaletskaya A, Dionne CA, Kedersha NL, Vater CA et al. A cytomegalovirus-encoded mitochondria-localized inhibitor of apoptosis structurally unrelated to bcl-2. *Proc Natl Acad Sci USA* 1999; **96**: 12536–12541.
9. Wasilenko ST, Stewart TL, Meyers AF, Barry M. Vaccinia virus encodes a previously uncharacterized mitochondrial-associated inhibitor of apoptosis. *Proc Natl Acad Sci USA* 2003; **100**: 14345–14350.
10. Fischer SF, Ludwig H, Holzapfel J, Kvansakul M, Chen L, Huang DCS et al. Modified vaccinia virus ankara protein F1L is a novel BH3-domain binding protein and acts together with the early viral protein E3L to block virus-associated apoptosis. *Cell Death Differ* 2006; **13**: 109–118.
11. Kvansakul M, van Delft MF, Lee EF, Gulbis JM, Fairlie WD, Huang DC et al. A structural viral mimic of prosurvival bcl-2: a pivotal role for sequestering proapoptotic bax and bak. *Mol Cell* 2007; **25**: 933–942.
12. Aoyagi M, Zhai D, Jin C, Aleshin AE, Stec B, Reed JC et al. Vaccinia virus N1L protein resembles a B cell lymphoma-2 (Bcl-2) family protein. *Protein Sci* 2007; **16**: 118–124.
13. Cooray S, Bahar MW, Abrescia NG, McVey CE, Bartlett NW, Chen RA et al. Functional and structural studies of the vaccinia virus virulence factor N1 reveal a Bcl-2-like anti-apoptotic protein. *J Gen Virol* 2007; **88** (Part 6): 1656–1666.
14. Bartlett N, Symons JA, Tscharke DC, Smith GL. The vaccinia virus N1L protein is an intracellular homodimer that promotes virulence. *J Gen Virol* 2002; **83** (Part 8): 1965–1976.
15. Wasilenko ST, Banadyga L, Bond D, Barry M. The vaccinia virus F1L protein interacts with the proapoptotic protein Bak and inhibits Bak activation. *J Virol* 2005; **79**: 14031–14043.
16. Taylor JM, Quilty D, Banadyga L, Barry M. The vaccinia virus protein F1L interacts with Bim and inhibits activation of the pro-apoptotic protein Bax. *J Biol Chem* 2006; **281**: 39728–39739.
17. Postigo A, Cross JR, Downward J, Way M. Interaction of F1L with the BH3 domain of Bak is responsible for inhibiting vaccinia-induced apoptosis. *Cell Death Differ* 2006; **13**: 1651–1662.
18. Bennett MJ, Schlunegger MP, Eisenberg D. 3D domain swapping: a mechanism for oligomer assembly. *Protein Sci* 1995; **4**: 2455–2468.
19. Muchmore SW, Sattler M, Liang H, Meadows RP, Harlan JE, Yoon HS et al. X-ray and NMR structure of human Bcl-x_L, an inhibitor of programmed cell death. *Nature* 1996; **381**: 335–341.
20. Czabotar PE, Lee EF, van Delft MF, Day CL, Smith BJ, Huang DC et al. Structural insights into the degradation of Mcl-1 induced by BH3 domains. *Proc Natl Acad Sci USA* 2007; **104**: 6217–6222.
21. Oberstein A, Jeffrey PD, Shi Y. Crystal structure of the Bcl-XL–Beclin 1 peptide complex: Beclin 1 is a novel BH3-only protein. *J Biol Chem* 2007; **282**: 13123–13132.
22. O'Neill JW, Manion MK, Maguire B, Hockenbery DM. BCL-XL dimerization by three-dimensional domain swapping. *J Mol Biol* 2006; **356**: 367–381.
23. Hsu YT, Youle RJ. Nonionic detergents induce dimerization among members of the Bcl-2 family. *J Biol Chem* 1997; **272**: 13829–13834.
24. Cartron PF, Gallenne T, Bougras G, Gautier F, Manero F, Vusio P et al. The first alpha helix of Bax plays a necessary role in its ligand-induced activation by the BH3-only proteins Bid and PUMA. *Mol Cell* 2004; **16**: 807–818.
25. Hinds MG, Smits C, Fredericks-Short R, Risk JM, Bailey M, Huang DC et al. Bim, Bad and Bmf: intrinsically unstructured BH3-only proteins that undergo a localized conformational change upon binding to prosurvival Bcl-2 targets. *Cell Death Differ* 2007; **14**: 128–136.
26. O'Connor L, Strasser A, O'Reilly LA, Hausmann G, Adams JM, Cory S et al. Bim: a novel member of the Bcl-2 family that promotes apoptosis. *EMBO J* 1998; **17**: 384–395.
27. Moldoveanu T, Liu Q, Tocilj A, Watson M, Shore G, Gehring K. The X-ray structure of a BAK homodimer reveals an inhibitory zinc binding site. *Mol Cell* 2006; **24**: 677–688.
28. Willis SN, Chen L, Dewson G, Wei A, Naik E, Fletcher JI et al. Pro-apoptotic Bak is sequestered by Mc1-1 and Bcl-xL, but not Bcl-2, until displaced by BH3-only proteins. *Genes Dev* 2005; **19**: 1294–1305.
29. Stewart TL, Wasilenko ST, Barry M. Vaccinia virus F1L protein is a tail-anchored protein that functions at the mitochondria to inhibit apoptosis. *J Virol* 2005; **79**: 1084–1098.
30. Zha H, Aime-Sempe C, Sato T, Reed JC. Proapoptotic protein Bax heterodimerizes with Bcl-2 and homodimerizes with Bax via a novel domain (BH3) distinct from BH1 and BH2. *J Biol Chem* 1996; **271**: 7440–7444.
31. Sugioka R, Shimizu S, Funatsu T, Tamagawa H, Sawa Y, Kawakami T et al. BH4-domain peptide from Bcl-xL exerts anti-apoptotic activity *in vivo*. *Oncogene* 2003; **22**: 8432–8440.
32. Altmann M, Hammerschmidt W. Epstein–Barr virus provides a new paradigm: a requirement for the immediate inhibition of apoptosis. *PLoS Biol* 2005; **3**: e404.
33. Chen L, Willis SN, Wei A, Smith BJ, Fletcher JI, Hinds MG et al. Differential targeting of pro-survival Bcl-2 proteins by their BH3-only ligands allows complementary apoptotic function. *Mol Cell* 2005; **17**: 393–403.

34. Oltersdorf T, Elmore SW, Shoemaker AR, Armstrong RC, Augeri DJ, Belli BA *et al.* An inhibitor of Bcl-2 family proteins induces regression of solid tumours. *Nature* 2005; **435**: 677–681.

35. Lee EF, Czabotar PE, Smith BJ, Deshayes K, Zobel K, Colman PM *et al.* Crystal structure of ABT-737 complexed with Bcl-xL: implications for selectivity of antagonists of the Bcl-2 family. *Cell Death Differ* 2007; **14**: 1711–1713.

36. Kaiser J. Smallpox vaccine. A tame virus runs amok. *Science* 2007; **316**: 1418–1419.

37. Emsley P, Cowtan K. Coot: model-building tools for molecular graphics. *Acta Crystallogr* 2004; **60** (Part 12): 2126–2132.

38. Laue TM, Shah BD, Ridgeway TM, Pelletier SL. Computer-aided interpretation of analytical sedimentation data for proteins In: Harding SE *et al.* (eds). *Analytical Ultracentrifugation in Biochemistry and Polymer Science*. The Royal Society of Chemistry: Cambridge, 1992, pp 90–125.

39. Hinds MG, Lackmann M, Skea GL, Harrison PJ, Huang DC, Day CL. The structure of Bcl-w reveals a role for the C-terminal residues in modulating biological activity. *EMBO J* 2003; **22**: 1497–1507.

40. Berman HM, Westbrook J, Feng Z, Gilliland G, Bhat TN, Weissig H *et al.* The protein data bank. *Nucleic Acids Res* 2000; **28**: 235–242.

Supplementary Information accompanies the paper on Cell Death and Differentiation website (http://www.nature.com/cdd)